Chapter 3
Large-Eddy Simulation of Smooth Channel Flow with a Stochastic Wall Model

Livia S. Freire

Abstract Large Eddy Simulation (LES) is a useful tool in the study of smooth channel flows of high Reynolds number, but when the domain is large enough computational cost restricts the correct representation of the viscous sublayer. In this study, we test the use of a one-dimensional stochastic model (ODT) as an alternative to simulate the flow close to the wall within the LES. This approach comprises the use of one independent ODT (a vertical line) inside each LES grid close to the wall, driven by the LES at the top and providing the lower boundary condition to the LES (two-way coupling). Results of mean velocity and total stress for $\mathrm{Re}_\tau = 590$ and 5200 are similar to Direct Numerical Simulation, and they have the correct order of magnitude for velocity variances.

Keywords Large-eddy simulation · One-dimensional turbulence · Smooth channel flow

3.1 Introduction

Smooth, pressure-driven channel flows correspond to one of the classical problems highly studied in the field of turbulence. In addition to its relative simplicity in terms of dimensional analysis, combined with many interesting features due to the wall-blockage effect, channel flows are present in a diverse set of applications in the environment (e.g., rivers and the atmospheric boundary layer) and industry (e.g., rectangular ducts).

In this study, we consider a channel with no lateral walls and with a distance δ from the bottom wall to the free stream at the top. The flow is fully developed, stationary, and horizontally homogeneous, and the *mean* flow is parallel to the wall (in the streamwise direction x). Statistics of the flow change only in the vertical direction, y, and the bottom wall is smooth, i.e., the velocity vector $\overrightarrow{u} = \langle u, v, w \rangle$ goes to zero at $y = 0$ (u, v, and w correspond to streamwise, vertical, and spanwise

L. S. Freire (✉)
Instituto de Ciências Matemáticas e de Computação, University of São Paulo, São Carlos, Brazil
e-mail: liviafreire@usp.br

H. F. Meier et al. (eds.), *Advances in Turbulence*, ABCM Series on Mechanical Sciences and Engineering, https://doi.org/10.1007/978-3-031-25990-6_3

velocities, respectively). From the continuity and momentum equations, it can be shown that the total stress

$$\tau(y) \equiv \rho\nu\frac{d\overline{u}}{dy} - \rho\overline{u'v'} \tag{1}$$

varies linearly with y because $d\tau/dy$ is constant (Pope 2000). In Eq. (1) ρ and ν are the fluid density and kinematic viscosity, respectively (both assumed as constants), over bars correspond to Reynolds average, and primes are the fluctuating part. The total stress is the sum of the viscous stress (first term on the RHS of Eq. (1)) and the Reynolds stress (second term). Noting that $\tau(y = \delta) = 0$, due to the free stream condition with no stress (similarly if considered an axisymmetric flow with another wall at $y = 2\delta$), we have that

$$\tau(y) = \tau_w\left(1 - \frac{y}{\delta}\right), \tag{2}$$

were τ_w is the shear stress at the wall. Since at the wall $u = v = 0$, $\tau_w = \rho\nu(d\overline{u}/dy)|_{y=0}$. A velocity scale known as *friction velocity* can be defined from τ_w, namely $u_\tau \equiv (\tau_w/\rho)^{1/2}$, which allows the definition of a friction Reynolds number $\mathrm{Re}_\tau = u_\tau\delta/\nu$. In addition, u_τ and ν can be used as viscous (or wall) scales to define nondimensional variables such as $u^+ = \overline{u}/u_\tau$ and $y^+ = yu_\tau/\nu$.

Figure 1 shows the statistics of smooth channel flows from Direct Numerical Simulation (DNS, the numerical solution of the Navier–Stokes equation) with $\mathrm{Re}_\tau = 590$ (from Moser et al. 1999) and $\mathrm{Re}_\tau = 5200$ (from Lee and Moser 2015). Notice the linear behavior predicted by Eq. (2) for $\tau(y)$ in Fig. 1f (it goes from 1 to 0 when normalized by u_τ), which is a signature that all assumptions are met by the simulation, including the steady-state condition. In terms of dimensional analysis, the flow can be divided into two layers (Pope 2000): (i) the inner layer ($y/\delta < 0.1$), where u_τ and y^+ are the dominant scales (white background in Fig. 1a–c) and (ii) the outer layer ($y/\delta > 0.1$), where u_b and δ are the dominant scales (grey background in Fig. 1a–c). The inner layer can be further subdivided into three sublayers: (i) the viscous sublayer ($y^+ < 5$), where the viscous stress dominates over the Reynolds stress and $u^+ = y^+$; (ii) the logarithmic layer ($30 < y^+ < 200$) where the Reynolds stress dominates over the viscous stress and $u^+ = \log y^+/\kappa + B$; and (iii) the buffer sublayer where both viscous and Reynolds stresses are relevant (see Fig. 1c for the relative importance of each stress). These equations for the nondimensional mean streamwise velocity (u^+) come from dimensional analysis, and the values of the constants $\kappa = 0.4$ and $B = 5.2$ were obtained experimentally (Pope 2000).

The analysis and equations described above and corroborated by experiments and DNS set the overall picture of canonical channel flows. Some interesting features can be observed when increasing the Reynolds number of the flow: in wall units (y^+), the inner layer remains the same (same viscous stress in Fig. 1c) and the outer layer increases in length, presenting a region with higher streamwise velocity (Fig. 1a). Variances peak at the buffer or logarithmic sublayers, and their values increase with

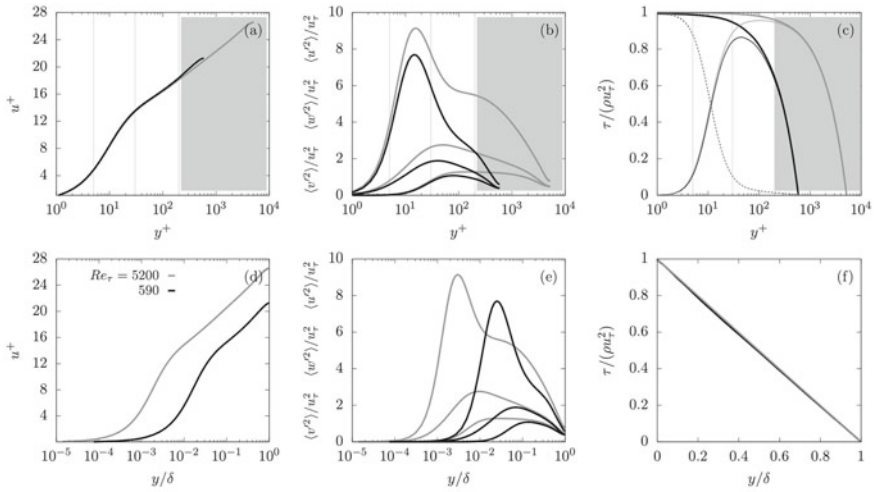

Fig. 1 Direct Numerical Simulation of smooth channel flows with $\mathrm{Re}_\tau = 590$ (black lines, from Moser et al. 1999) and $\mathrm{Re}_\tau = 5200$ (gray lines, from Lee and Moser 2015); **a** and **d**: mean streamwise velocity, **b** and **e**: variances of streamwise (upper lines), spanwise (middle lines) and vertical (lower lines) velocities, **c** and **f**: total (thick lines), viscous (dotted lines) and Reynolds (thin lines) stresses; **a**–**c** are displayed as a function of $y^+ = yu_\tau/\nu$, whereas **d**–**f** use y/δ. In **a**–**c** vertical lines separate the viscous, buffer, and logarithmic layers (from left to right); the outer layer corresponds to the gray area

Re_τ at all layers except the viscous sublayer (Fig. 1b). When looking at these statistics as a function of the distance from the wall (y/δ), the important feature to notice is that as Re_τ increases, the inner layer is "pushed" closer to the wall (Fig. 1d, e).

Simulation of $\mathrm{Re}_\tau = 5200$ from Lee and Moser (2015) already corresponds to one of the highest Re_τ values allowed by current computational capabilities for DNS, but some applications (such as the atmospheric boundary layer) require values of Re_τ one order of magnitude higher or more. In these situations, an alternative is to use another numerical tool known as Large-Eddy Simulation (LES), in which all variables are filtered for small-scale removal, significantly reducing the computational cost while maintaining most of the kinetic energy of the flow.

The governing equations of LES are obtained by filtering Navier–Stokes and continuity equations, which (for incompressible flow) corresponds to (Pope 2000)

$$\frac{\partial \tilde{u}_i}{\partial t} + \frac{\partial \widetilde{u_i u_j}}{\partial x_j} = -\frac{1}{\rho}\frac{\partial \tilde{p}}{\partial x_i} + \nu \frac{\partial^2 \tilde{u}_i}{\partial x_j \partial x_j} + F_i, \tag{3}$$

$$\frac{\partial \tilde{u}_i}{\partial x_i} = 0, \tag{4}$$

where $\tilde{u}_i$ is the filtered velocity field, $\tilde{p}$ is the filtered pressure field, and F_i is the mean streamwise pressure forcing (traditional index notation is used). In order to close this

set of equations, the second term on the LHS of Eq. (3) needs to be rewritten as a function of the resolved velocity $\tilde{u}_i$ and pressure $\tilde{p}$. By defining the residual stress tensor and the residual kinetic energy as

$$\tau_{ij}^R \equiv \widetilde{u_i u_j} - \tilde{u}_i \tilde{u}_j, \tag{5}$$

$$e^R \equiv \frac{1}{2}\tau_{ii}^R, \tag{6}$$

it is possible to write

$$\widetilde{u_i u_j} = \tau_{ij} + \frac{2}{3} e^R \delta_{ij} + \tilde{u}_i \tilde{u}_j, \tag{7}$$

where τ_{ij} is the anisotropic part of the residual stress tensor ($\tau_{ij} = \tau_{ij}^R - 2e^R\delta_{ij}/3$), also known as subgrid-scale (SGS) stress tensor. The final Navier–Stokes equation for LES can be written as (Bou-Zeid et al. 2005)

$$\frac{\partial \tilde{u}_i}{\partial t} + \frac{\partial \tilde{u}_i \tilde{u}_j}{\partial x_j} = -\frac{1}{\rho}\frac{\partial \tilde{p}^*}{\partial x_i} + \frac{\partial \tau_{ij}}{\partial x_j} + F_i, \tag{8}$$

where $\tilde{p}^* = \tilde{p} + \frac{2}{3}\rho e^R$ is a modified pressure. Note that because molecular viscosity can be neglected in the resolved scales of high Reynolds number flows, it was removed from Eq. (8). The impact of the unsolved part of the flow on the resolved velocity field is represented by τ_{ij}, which is the term that needs to be parameterized as a function of the resolved velocity field. A diverse set of parameterizations, known as SGS models, has been developed for different applications and numerical approaches, most of them based on the eddy-viscosity and mixing-length assumptions.

When using LES to simulate smooth channel flows, it is possible to adopt a vertically stretched grid so that the first grid points are within the viscous sublayer, and a no-slip boundary condition can be enforced at the wall (e.g., Lund et al. 1998; Schlatter et al. 2010). This option, however, restricts the size of the domain, because the number of points to be used in the vertical direction is limited by the computational cost, the stretching function, and the assumptions of the SGS model used. Another option is to have the lowest LES grid points at the logarithmic region, and to use the log-law equation for the mean flow in this region ($u^+ = \log y^+/\kappa + B$) to relate the instantaneous streamwise velocity at the lowest grid point to the expected velocity gradient at the wall (used as a Neumann boundary condition). This is done through the value of u_τ, which carries the value of $d\overline{u}/dy|_{y=0}$ (see prior definitions of u^+, u_τ and τ_w). The main issue with this approach is that the log-law is true for the *mean* streamwise velocity $u^+ = \overline{u}/u_\tau$, but not for the instantaneous filtered velocity $\tilde{u}$ being resolved by the LES. Therefore, errors from this misuse of the log-law are present. Nevertheless, this method provides reasonable results, and it is widely used in cases in which the size of the domain is too large for the stretched grid approach (e.g., Bou-Zeid et al. 2005; Brasseur and Wei 2010).

An alternative to the use of the log-law when the first LES grid points are in the logarithmic sublayer was proposed by Schmidt et al. (2003). In this approach, a one-dimensional stochastic model is used to simulate the instantaneous flow field in the viscous and buffer sublayer, two-way coupled with the resolved flow field in the LES. In this study, we reproduce this method in a different LES code, comparing it again with DNS results of $\mathrm{Re}_\tau = 590$ by Moser et al. (1999) and performing a new comparison with the most recent DNS results of $\mathrm{Re}_\tau = 5200$ by Lee and Moser (2015). Positive and negative aspects of this method are discussed, and future applications for the model are envisioned.

3.2 Methods

3.2.1 One-Dimensional Stochastic Model

The one-dimensional stochastic model used in this study, known as ODT (One-Dimensional Turbulence model), was developed by Kerstein (1999) and successfully used as a stand-alone model to simulate different types of turbulent flows, including homogeneous turbulence, shear layers, buoyancy-driven flows (Kerstein 1999), mixing-layer and wakes (Kerstein et al. 2001), jet diffusion flames (Echekki et al. 2001), the stable atmospheric boundary layer (Kerstein and Wunsch 2006), particle dispersion in homogeneous flows (Sun et al. 2014) and flow through plant canopies (Freire and Chamecki 2018). The model corresponds to the one-dimensional diffusion equation of all variables of interest (which in this study are the three velocity components, but temperature, gas, and particle concentration can be included in the same way), i.e.,

$$\frac{\partial u_i}{\partial t} = \nu \frac{\partial^2 u_i}{\partial y^2} + F_i + stochastic\,eddies \tag{9}$$

where *stochastic eddies* correspond to the effect of three-dimensional turbulence in this one-dimensional field. The simulation is performed by evolving the diffusion equation in time, and at each time-step, a *stochastic eddy* is selected from a probability distribution of eddy size and location in the domain. When a *stochastic eddy* is selected, all variables at the position y within the eddy are replaced by the value of the same variable at the position $M(y)$. This mapping function is a model for advection, mixing the variables and creating small-scale fluctuations in such a way that mimics the energy cascade of turbulent flows. It is conservative (i.e., it preserves the total amount of the quantity being transported) and it does not introduce discontinuities. Mathematically, it is defined as

$$M(y) = y_b + \begin{cases} 3(y - y_b), & \text{if } y_b \le y \le (y_b + l/3), \\ 2l - 3(y - y_b), & \text{if } (y_b + l/3) \le y \le (y_b + 2l/3), \\ 3(y - y_b) - 2l, & \text{if } (y_b + 2l/3) \le y \le (y_b + l), \\ y - y_b, & \text{otherwise}, \end{cases} \tag{10}$$

where l and y_b are the size and bottom position of the eddy, respectively. As described by Kerstein and Wunsch (2006), the mapping function "takes a line segment, shrinks it to a third of its original length, and then places three copies on the original domain. The middle copy is reversed, which maintains continuity of advected fields and introduces the rotational folding effect of turbulent eddy motion." In addition to this mixing effect, when a *stochastic eddy* is selected, a second term creates redistribution of energy among velocity components, mimicking a pressure-induced tendency toward isotropy on the flow. The final model for the occurrence of *stochastic eddies* is

$$u_i(y) \rightarrow u_i(M(y)) + c_i(y - M(y)), \tag{11}$$

where c_i is the amplitude of the energy redistribution (calculated from the flow energy within the eddy). For more details on its calculation, see Kerstein (1999) and Kerstein et al. (2001).

The final piece of information needed for the ODT is the probability distribution of eddy size and location, $\lambda(l, y_b, t)$, which also evolves in time with the flow. It is calculated as proportional to the instantaneous amount of kinetic and potential energy in the flow (through dimensional analysis), adding another physical aspect to the stochastic model. For example, regions of high shear will have a higher probability of having *stochastic eddies*. A proportionality constant C_λ is used to regulate the number of eddies for a given amount of energy, effectively setting the turbulence intensity. Another constant, Z_λ, adjusts the damping effect of viscosity, because any eddy with a time scale longer than the viscous time scale should be prohibited. The values of C_λ and Z_λ are the only tunable parameters of the model, which are usually different for different types of flows, but they are not expected to vary with Re_τ. A detailed description of λ and its mathematical formulation can also be found in Kerstein (1999) and Kerstein et al. (2001).

When used as a bottom boundary condition for the LES, an independent ODT model is inserted inside each LES grid next to the wall. In this case, each ODT corresponds to a vertical line centered at the LES grid, refining the flow field in the vertical direction from the wall to the top of the grid. The LES velocity field provides a top boundary condition to the ODT, and the ODT provides the momentum flux across the first and second grid layers as a bottom boundary condition for the LES, which results in an instantaneous two-way coupling between the models.

Table 1 Simulation parameters for LES and ODT

	$\mathrm{Re}_\tau = 590$	$\mathrm{Re}_\tau = 5200$
Domain size ($X \times Y \times Z$)	$2\pi\delta \times \delta \times 2\pi\delta$	$2\pi\delta \times \delta \times 2\pi\delta$
Number of grid points ($N_x \times N_y \times N_z$, N_{ODT})	$32 \times 16 \times 32$, 32	$32 \times 32 \times 32$, 96
Mean pressure gradient force ($F_i = \langle(1/\rho)(d\overline{p}/dx), 0, 0\rangle$)	$\langle u_\tau^2/\delta, 0, 0\rangle$	$\langle u_\tau^2/\delta, 0, 0\rangle$
Simulation time step (Δt)	$0.0005\delta/u_\tau$	$0.0005\delta/u_\tau$
Number of simulation time steps (N_t)	100, 000	100, 000
Eddy rate distribution parameters (C_λ, Z_λ)	23, 15	23, 15

3.2.2 Large-Eddy Simulation Code

The LES code used in this study solves the filtered Navier–Stokes equation in a vertically-staggered grid with fixed size, in which the first grid points are located in the logarithmic sublayer. The numerical discretization combines a fully dealiased pseudo-spectral method in the horizontal directions and a second-order centered finite difference in the vertical direction. The fully explicit second-order Adams–Bashforth scheme is used for time integration. The SGS model is the planar averaging, scale-invariant dynamic model (Germano et al. 1991). More details of the code can be found in Bou-Zeid et al. (2005). A constant mean pressure gradient force is imposed in the streamwise direction and horizontal boundary conditions are periodic, while a stress-free boundary condition is applied at the top of the domain.

3.2.3 Simulation Setup

Two simulations are tested here, corresponding to $\mathrm{Re}_\tau = 590$ and 5200. Simulation parameters are listed in Table 1. Both simulations were run for 50 eddy turnover times (defined as δ/u_τ), and results presented in the next section correspond to the averaging of the last 15 eddy turnover times.

3.3 Results

Figure 2 shows the results of flow statistics for the two Re_τ tested. After the adjustment of the parameters C_λ and Z_λ (by trial and error), the mean flow is well represented by the model, with ODT providing the velocity field in the viscous and buffer sublayers in the $\mathrm{Re}_\tau = 590$ case (Fig. 2a), and in most of the inner layer in the case

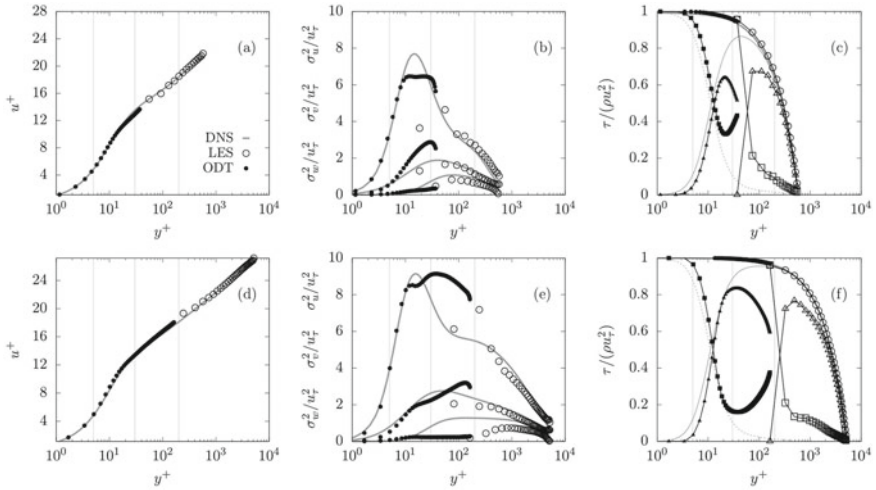

Fig. 2 Smooth channel flow simulation results from ODT-LES coupling for $\mathrm{Re}_\tau = 590$ (**a**–**c**) and $\mathrm{Re}_\tau = 5200$ (**d**–**f**); LES (ODT) results in empty (filled) symbols; gray lines correspond to DNS results; **a** and **d**: mean streamwise velocity, **b** and **e**: variances of streamwise (upper lines/symbols), spanwise (middle lines/symbols), and vertical (lower lines/symbols) velocities, **c** and **f**: total (circles), viscous and SGS (squares), and *stochastic eddies* and resolved (triangles) stresses

of $\mathrm{Re}_\tau = 5200$ (Fig. 2d). The fact that these tunable parameters do not change with Re_τ is useful in terms of the applicability of the model to different studies.

Overall, variances are well represented by the LES in the outer layer; this is also obtained when using wall models based on the log-law, and it is likely not significantly impacted by the use of the ODT. The variances at the viscous sublayer are also well represented by the ODT, but ODT results in the buffer and logarithmic sublayers show discrepancies when compared to DNS results (Fig. 2b, e). Even as a stand-alone model, variances from ODT are usually not correct, which has been consistently observed for different types of flows (Kerstein et al. 2001; Freire and Chamecki 2018). Nevertheless, having an estimate that has the correct order of magnitude can be useful in some applications where an instantaneous flow field close to the wall is needed.

Finally, stresses are well represented by the ODT-LES coupling. Note in Fig. 2c, f that the ODT viscous stress is similar to DNS values, and that the *stochastic eddies* emulate the Reynolds stress in the viscous and part of the buffer sublayers. The sum of them gives the correct total stress at these layers, and it provides the value of the stress in the second LES grid point (which enters as an SGS stress). The total stress in the LES is divided into SGS and resolved parts (both corresponding to the Reynolds stress), and no viscous stress exists as it is negligible in this part of the domain. As expected, the total stress matches the linear profile (from theory and DNS) in both ODT and LES parts, indicating a well-developed, steady-state simulation.

3.4 Conclusion

In this study, we tested the use of a one-dimensional stochastic model as an alternative to simulate, in LES, the lowest part of the inner layer of a smooth channel flow. This approach provides good results for mean velocity and total stress, in addition to reasonable results (in terms of order of magnitude) for the variances of the flow. Despite the errors in variances, this option is likely more robust than the use of the log-law as a wall model for the instantaneous resolved velocity, given that the latter is an equation defined for the *mean* flow. The trade-off of this correction, however, comes in a significant increase in the computational cost of the simulation. Perhaps the application in which the ODT-LES coupling will be most useful is when the information of the instantaneous flow field very close to the wall is needed in addition to a large domain (too large for the stretched grid approach), such as studies of particle transport at the surface of the atmospheric boundary layer under conditions of strong convective flows.

Acknowledgements LF was funded by São Paulo Research Foundation (FAPESP, Brazil) Grant No. 2018/24284-1. This research was carried out using the computational resources of the Center for Mathematical Sciences Applied to Industry (CeMEAI) also funded by FAPESP (Grant No. 2013/07375-0).

References

Bou-Zeid E, Meneveau C, Parlange M (2005) A scale-dependent Lagrangian dynamic model for large eddy simulation of complex turbulent flows. Phys Fluids 17(2):025105

Brasseur JG, Wei T (2010) Designing large-eddy simulation of the turbulent boundary layer to capture law-of-the-wall scaling. Phys Fluids 22(2):021303

Echekki T, Kerstein AR, Dreeben TD, Chen JY (2001) One-dimensional turbulence simulation of turbulent jet diffusion flames: model formulation and illustrative applications. Combust Flame 125(3):1083–1105

Freire LS, Chamecki M (2018) A one-dimensional stochastic model of turbulence within and above plant canopies. Agric For Meteorol 250–251:9–23

Germano M, Piomelli U, Moin P, Cabot WH (1991) A dynamic subgrid-scale eddy viscosity model. Phys Fluids A 3(7):1760–1765

Kerstein AR (1999) One-dimensional turbulence: model formulation and application to homogeneous turbulence, shear flows, and buoyant stratified flows. J Fluid Mech 392:277–334

Kerstein AR, Wunsch S (2006) Simulation of a stably stratified atmospheric boundary layer using one-dimensional turbulence. Bound-Layer Meteorol 118(2):325–356

Kerstein A, Ashurst WT, Wunsch S, Nilsen V (2001) One-dimensional turbulence: vector formulation and application to free shear flows. J Fluid Mech 447:85–109

Lee M, Moser RD (2015) Direct numerical simulation of turbulent channel flow up to $\mathrm{Re}_\tau \approx 5200$. J Fluid Mech 774:395–415

Lund TS, Wu X, Squires KD (1998) Generation of turbulent inflow data for spatially-developing boundary layer simulations. J Comput Phys 140(2):233–258

Moser RD, Kim J, Mansour NN (1999) Direct numerical simulation of turbulent channel flow up to $\mathrm{Re}_\tau = 590$. Phys Fluids 11(4):943–945

Pope SB (2000) Turbulent flows. Cambridge University Press
Schlatter P, Li Q, Brethouwer G, Johansson AV, Henningson DS (2010) Simulations of spatially evolving turbulent boundary layers up to $Re_\theta = 4300$. Int J Heat Fluid Flow 31(3):251–261
Schmidt RC, Kerstein AR, Wunsch S, Nilsen V (2003) Near-wall LES closure based on one-dimensional turbulence modeling. J Comput Phys 186(1):317–355
Sun G, Lignell DO, Hewson JC, Gin CR (2014) Particle dispersion in homogeneous turbulence using the one-dimensional turbulence model. Phys Fluids 26(10):103301